Features of magnetoresistance and magnetic properties in $Bi_{95.69}Mn_{3.69}Fe_{0.62}$

A. V. Terekhov, K. Rogacki, A. L. Solovjov, A. N. Bludov, A. I. Prokhvatilov, V. V. Meleshko, I. V. Zolochevskii, E. V. Khristenko, J. Cwik, A. Los, A. D. Shevchenko, Z. D. Kovalyuk, and O. M. Ivasishin

---
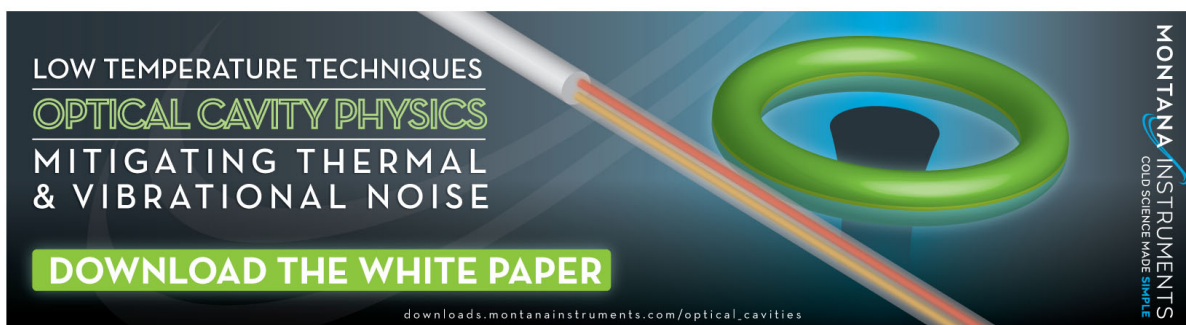
Articles you may be interested in

Berry phase in strained InSb whiskers
Low Temperature Physics **44**, 1189 (2018); 10.1063/1.5060974

Features of magnetoresistance and magnetic properties in Bi$_{95.69}$Mn$_{3.69}$Fe$_{0.62}$

A. V. Terekhov,[1,a)] K. Rogacki,[2] A. L. Solovjov,[1] A. N. Bludov,[1] A. I. Prokhvatilov,[1]
V. V. Meleshko,[1] I. V. Zolochevskii,[1] E. V. Khristenko,[1] J. Cwik,[2] A. Los,[2]
A. D. Shevchenko,[3] Z. D. Kovalyuk,[4] and O. M. Ivasishin[3]

[1]Verkin Institute for Low Temperature Physics and Engineering, Kharkov, Ukraine, 61103
[2]W. Trzebiatowski Institute for Low Temperatures & Structure Research PAS, P.O. Box 1410, 50–950,
Wroclaw, Poland
[3]Kurdyumov Institute for Metal Physics, Kiev, Ukraine, 03142
[4]I.M. Frantsevich Institute for Problems of Material Science, Chernivtsi, Ukraine, 58001

A study of textured, polycrystalline Bi$_{95.69}$Mn$_{3.69}$Fe$_{0.62}$ containing two phases: the bismuth matrix
and inclusions of the α-BiMn phase. It is shown that the anomalous behavior of the magnetization
temperature dependences can be linked to the reorientation transition of the Mn magnetic moments
in the α-BiMn phase, caused by the change in the sign of the magnetic anisotropy constant. It is
established that the temperature dependences of the electrical resistivity in a magnetic field are
non-monotonic, and that the magnetoresistance is positive in all temperature ranges, reaching
a maximum value of 3033% for a magnetic field of 140 kOe, when the magnetic field is
perpendicular to the transport current. A strong anisotropy of electrical resistivity is measured in a
magnetic field. It is assumed that the anomalous behavior of the electrical resistivity as a function
of temperature in Bi$_{95.69}$Mn$_{3.69}$Fe$_{0.62}$, as compared to pure bismuth, is linked to a change in the
overlap between the electron and the hole Fermi surfaces under the influence of α-BiMn phase
magnetism, as well as the magnitude and direction of the external magnetic field. *Published by AIP
Publishing.* https://doi.org/10.1063/1.5060969

Introduction

Bismuth possesses extraordinary electronic properties
and has thus been the subject of intense research for over 100
years. Among these properties are the small effective charge
carrier masses (about 10–2–10–1 of the free electron mass),
small number of charge carriers (about 10^{-5} electrons per
atom), large electron mean free path (can reach 1 mm), and a
Fermi energy E_F that is about a few hundredths of an electron
volt (in simple metals E_F is about several eV). Furthermore,
bismuth possesses both large dielectric (about 10^{-5}) and dia-
magnetic (∼100) permeabilities, as well as a g-factor
approaching 200. Owing to these properties, bismuth was the
first material in which the Shubnikov–De Haas and De Haas–
Van Alphen effects, large positive magnetoresistance, cyclo-
tron resonance in a metal, oscillatory magnetostriction,
undamped microwaves, as well as a variety of size effects [1,2]
were experimentally observed. For a long time it was believed
that bulk bismuth does not transition to a superconducting
state under normal pressure. However, recently, a group of
scientists from India discovered such a transition in single
crystal bismuth at ultra-low temperatures ($T_c \approx 0.5$ mK).[3]

Bismuth compounds also present a significant interest.
Among them, for example, is the high-temperature supercon-
ductor Bi$_2$Sr$_2$Ca$_2$Cu$_3$O$_{10+x}$ (BiSCCO, Bi-2223) with a super-
conducting transition temperature reaching 110 K[4] an alloy
of 88% Bi and 12% Sb that shows an anomalous magnetore-
sistance effect in magnetic fields,[5] and finally BiMn alloys
that occupy a special place among permanent magnets.[6,7]

BiMn is a ferromagnet with a high transition temperature
into the ferromagnetic state of $T_C \approx 640$ K. Solid solutions of
BiMn are interesting due to their high coercive force at room
temperature. With increasing temperature, it grows to values

exceeding the coercive forces of rare-earth permanent
magnets.[6,7] This fact, as well as the relative cheapness of
these materials vis-a-vis the rare-earth magnets, makes them
attractive for practical application in high-temperature work.

At the same time, even though a huge amount of work
exists on the magnetic properties of BiMn alloys, studies on
electric transport are extremely scarce. Our group has
recently observed colossal positive anisotropic magnetoresis-
tance in a Bi$_{95.69}$Mn$_{3.69}$Fe$_{0.62}$ alloy, for the first time.[8]

In this study, we continue to investigate the magnetore-
sistance in Bi$_{95.69}$Mn$_{3.69}$Fe$_{0.62}$, together with its structural
and magnetic properties, with the aim of shedding light on
the nature of the anomalies that are observed in its electrical
resistivity temperature dependences in a magnetic field.

Samples and experimental method

The starting materials for the samples were bismuth and
manganese with a purity of >99.999%. The vessels for syn-
thesis and crystal growth were graphitized quartz ampules
with a diameter of Ø 16–18 mm, evacuated to a residual pres-
sure of ∼10^{-2} Pa. The synthesis was carried out in a SUOL
horizontal tubular furnace. The alloy samples were obtained
by Bridgeman crystallization at a temperature of 630 K with a
growth rate of 1.5 mm/hr. Under such growth conditions, pro-
duction of single-crystal and coarse-grain textured samples is
possible. It is necessary to stabilize the furnace temperature in
order to grow quality materials (especially at the crystalliza-
tion front). This was accomplished using a RIF-101 tempera-
ture control unit with an accuracy of ± 0.5°C.

The final ingots were cylindrical in shape.
Measurements of electrical resistivity along the base of the

cylinder (perpendicular to the *c*-axis) were performed by cutting out parallelepiped samples with dimensions of approximately $7 \times 2 \times 2$ mm. To measure the magnetic properties, small samples weighing up to 10 mg were cut from these same parallelepipeds.

The grown samples were tested at room temperature using X-ray analysis on a DRON-3 diffractometer under K_α-radiation from a copper anode ($\lambda = 1.54178$ Å). A scanning electron microscope (SEM) was used to determine the quantitative elemental composition and to observe the microstructure.

The resistive and magnetoresistive measurements were performed using a standard four-probe circuit on an automated physical property measurement system (PPMS) from Quantum Design. Current and potential junctions were made with silver paste. The measurements were conducted in alternating current mode ($I = 30$ mA, $f = 17$ Hz) directed along the larger dimension of the sample, both without an applied field, and in transverse and longitudinal magnetic fields with magnitudes up to 140 kOe in the temperature range of 4.2-300 K.

The magnetization was measured on a vibrational magnetometer in a temperature range of 4.2-300 K in two regimes. In the first, the sample was cooled to 4.2 K without a field, after which the magnetic field was turned on and the magnetization was measured during heating (zero field cooling regime, ZFC). In the second regime, the magnetization was measured immediately in a field, as the sample was cooled from room temperature (field cooling regime, FC). The dynamic magnetic susceptibility $\chi'(\omega,T)$ and $\chi''(\omega,T)$ was measured in the same temperature range as the magnetization at alternating field frequencies ranging from 100 Hz to 10 kHz and an amplitude of 15 Oe. The magnetic field was oriented both along the base of the cylinder ($\mathbf{H} \perp \mathbf{c}$), as well as perpendicular to it ($\mathbf{H} \parallel \mathbf{c}$).

For these measurements, the constant magnetic field was supplied by a superconducting solenoid.

Experimental results and discussion

Structural studies

According to SEM results, the quantitative elemental composition of the obtained alloy was as follows: 95.69 at% Bi, 3.69 at%Mn, 0.62 at%Fe. Unfortunately, it was not possible to get a good enough slice of the surface at the fracture to obtain an adequate visualization of the microstructure. At the same time, considering the results of the quantitative analysis and matching them to the phase diagram of Bi-Mn solid solutions,[9] we can say with a large amount of certainty that the sample is a bismuth matrix with α-BiMn phase inclusions.

With the aim of obtaining information on the structure of the studied alloy, we also carried out X-ray diffraction studies on a DRON-3 diffractometer under K_α-radiation from a copper anode ($\lambda = 1.54178$ Å). The obtained X-ray diffraction spectra suggest polycrystallinity of the samples. It was determined that the polycrystalline material has a hexagonal lattice with parameters $a = 4.558$ Å, $c = 11.885$ Å, $\beta = 120°$, which are slightly larger than for pure bismuth ($a = 4.54$ Å, $c = 11.82$ Å, $\beta = 120°$). This suggests that the solid solution contains not only pure bismuth but also a weak solution of Mn atoms in the bismuth hexagonal lattice. At the same time, the presence of peak (202) in the diffraction spectra,

which is absent in bismuth, can suggest the presence of a small amount of the α-BiMn phase.[10] According to the phase diagram of Bi-Fe,[9] iron does not form intermetallic phases with bismuth, and therefore small amounts of individual iron inclusions exist in our compound.

The possible texture of the prepared samples was studied by analyzing the X-ray diffraction spectra of both the bulk alloy and its powders. The powders were obtained by grinding the bulk sample with a mechanical file. The X-ray diffractograms of the bulk and powdered samples are shown in Fig. 1, with the results of the processing presented in Table 1.

It is clear that the X-ray patterns of the bulk and the powdered sample are qualitatively similar and correspond well in hexagonal syngony. The polycrystalline sample and the powder have fairly close hexagonal lattice parameters: $a = 4.558$ Å, $c = 11.885$ Å, $\beta = 120°$ and $a = 4.5647$ Å, $c = 11.893$ Å, $\beta = 120°$, respectively. The integrated intensities of most of the diffraction lines are 20–70% higher for the powder than for the bulk sample. The intensities of the (202) lines are almost 2.5 times greater than the corresponding lines for the bulk alloy. The higher scattering intensity on the powdered sample is partially explained by the relaxation of the bulk sample macrostresses during the filing procedure. The observed anisotropy and the anomalously high differences between the intensities of individual lines (202), (104) and others (see Table 1) suggest the presence of a growth texture, which is closely related to the movement direction of the alloy crystallization front.

Magnetic studies

Our measurements of the temperature and magnetic-field dependences of the iron-free alloy $\text{Bi}_{88.08}\text{Mn}_{11.92}$ (to be published shortly) show that these dependences are in qualitative agreement with the $M(T)$ and $M(H)$ of the iron-containing alloy $\text{Bi}_{95.69}\text{Mn}_{3.69}\text{Fe}_{0.62}$ that is the subject of this study. Therefore, we will not discuss the impact of a small amount of iron on the bulk magnetic properties of $\text{Bi}_{95.69}\text{Mn}_{3.69}\text{Fe}_{0.62}$, and will assume that the magnetism in our case is generated solely by the α-BiMn phase inclusions. Our measurements of the $M(T)$ and $M(H)$ dependences for
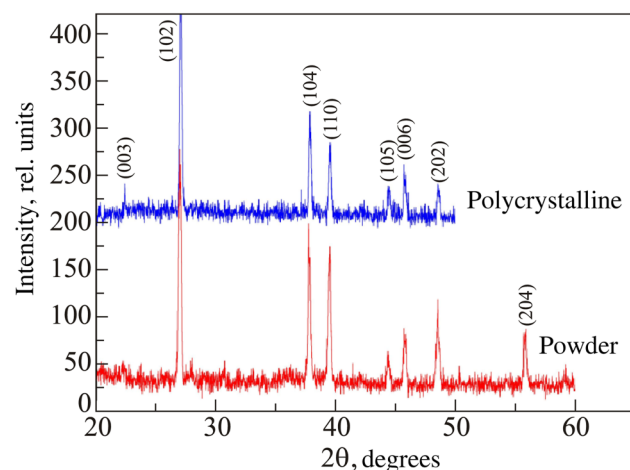

Fig. 1. X-Ray diffraction spectra of both the polycrystalline and the powdered $\text{Bi}_{95.69}\text{Mn}_{3.69}\text{Fe}_{0.62}$ alloy samples. The diffraction spectra were obtained at room temperature under K_α- radiation from a copper anode.

TABLE 1. Experimental (θ_0) and calculated (θ_C) X-ray reflection angles from both the polycrystalline and powdered alloy samples of $Bi_{95.69}Mn_{3.69}Fe_{0.62}$. The calculated values ($2\theta_C$) are determined using the obtained parameters of the hexagonal lattice with $P6_3/mmm$ symmetry. I_{area} and FWHM are the integrated intensity and the half-width of the X-ray reflections.

Polycrystalline sample obtained by the Bridgeman method						Powdered sample obtained by filing the bulk polycrystalline sample					
h k l	$2\theta_0$	$2\theta_C$	Δ	I_{area}	FWHM	h k l	$2\theta_0$	$2\theta_C$	Δ	I_{area}	FWHM
1 0 2	27.09	27.12	0.03	53.58	0.199	1 0 2	27	27.08	0.09	66.25	0.262
1 0 4	37.88	37.90	0.02	22.02	0.222	1 0 4	37.81	37.86	0.05	38.17	0.261
1 1 0	39.54	39.54	0.00	16.29	0.227	1 1 0	39.49	39.48	0.01	39.49	0.269
1 0 5	44.49	44.49	0.00	6.82	0.224	1 0 5	44.44	44.45	0.01	8.21	0.299
0 0 6	45.81	45.81	0.01	10.67	0.260	0 0 6	45.80	45.77	0.03	15.86	0.292
2 0 2	48.61	48.61	0.01	6.91	0.215	2 0 2	48.56	48.53	0.02	24.35	0.336

field directions **H** ∥ **c** and **H** ⊥ **c** were in good agreement. At the same time, according to Ref. 7, these dependences, which were measured along different directions in the BiMn single crystals, differed significantly with respect to magnetization magnitude. One possible explanation for this discrepancy could be the fact that in our case, the total magnetic contribution from the α-BiMn phase to the sample volume is similar to what is observed in ordinary non-textured polycrystalline BiMn, in which all of the magnetization directions are approximately equal. Our study shows that the contribution of the α-BiMn phase to the magnetic properties of the $Bi_{95.69}Mn_{3.69}Fe_{0.62}$ is defining.

Figure 2 shows the temperature dependence of the magnetization $M(T)$ measured in magnetic fields of 0.2, 4, 10 and 30 kOe. $M(T)$ undergoes significant changes with an increasing magnetic field. At 0.2 and 4 kOe [Fig. 2(a), (b)] maxima are observed at 105 and 85 K, respectively. These features are absent for field values of 10 and 30 kOe [Fig. 2(c), (d)]. Previously, the authors of Refs. 7 and 11 studied the magnetic properties of Bi-Mn solid solutions with α-BiMn phase content much larger than ours (40, 45 and 50at%Mn) and found a maximum along $M(T)$ at 90 K. They explained the presence of this anomaly by the reorientation of the manganese magnetic moments with decreasing temperature. It is assumed that the spins of the Mn atoms change their direction from perpendicular to parallel with respect to the crystallographic axis *c*, in the temperature range of 30-150 K. It is likely that such an explanation for the peak along *M(T)* can also be applicable in our case. A detailed study of the magnetization temperature dependence for the 0.2 kOe field shows a divergence between the curves measured in the FC and ZFC modes, in the vicinity of the maximum. Such behavior is often observed in spin glasses [12–14] (disordered magnets in which magnetic moment orientation is not spatially periodic, and the magnetic moments themselves, in contrast to paramagnets, do not fluctuate in time, i.e. it is as though they are "frozen"), cluster spin glasses [15–17] (systems with "frozen" interacting ferromagnetic clusters), or phase-segregated systems with ferromagnetic inclusions that form a superparamagnet.[14,17–19] In our case, α-BiMn phase inclusions, depending on their size and distribution throughout sample volume, can behave both as superparamagnetic particles and as cluster spin glasses. In the first, the exchange interaction between individual inclusions is negligible, whereas in the second, it becomes pronounced. When studying spin glasses and superparamagnets, one measures the dynamic properties (for example magnetic susceptibility in

an alternating field), since, based on the literature,[12–14] it is known that in a certain way, the location and the magnitude of the maximum along the temperature dependence of the dynamic susceptibility in these materials depends on the
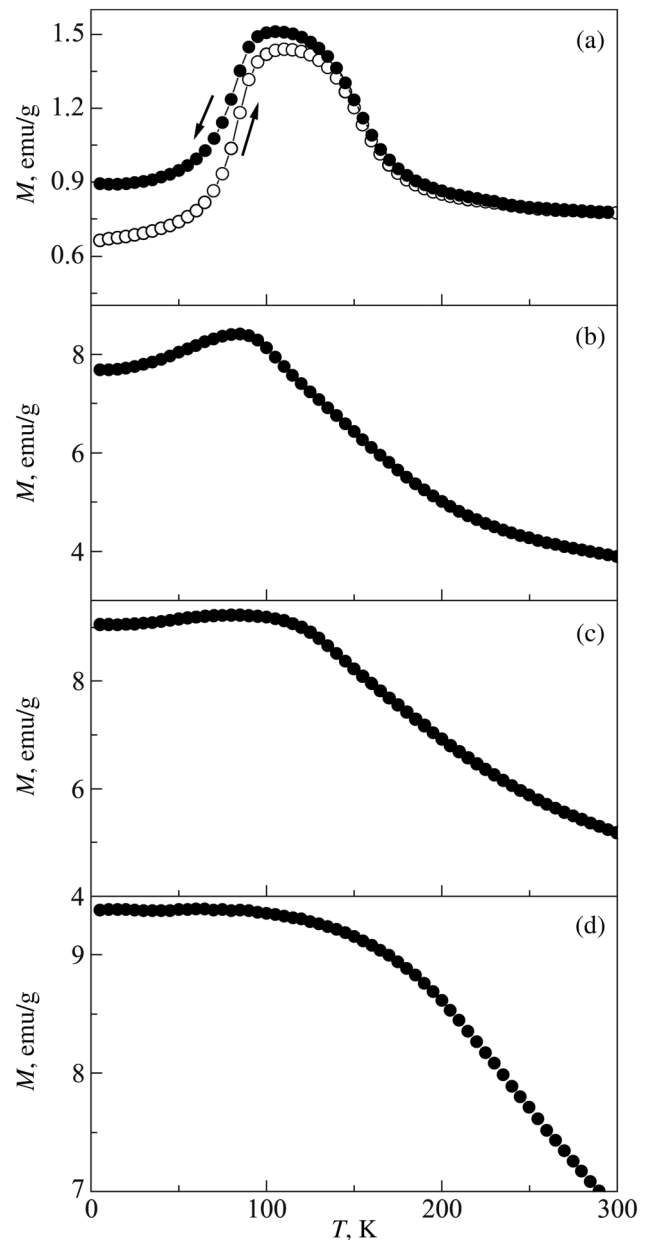

Fig. 2. $M(T)$ dependence of $Bi_{95.69}Mn_{3.69}Fe_{0.62}$ measured in magnetic fields of 0.2 (a), 4 (b), 10 (c) and 30 (d) kOe. The symbols denote measurements in the ZFC (○) and FC (●) regimes.
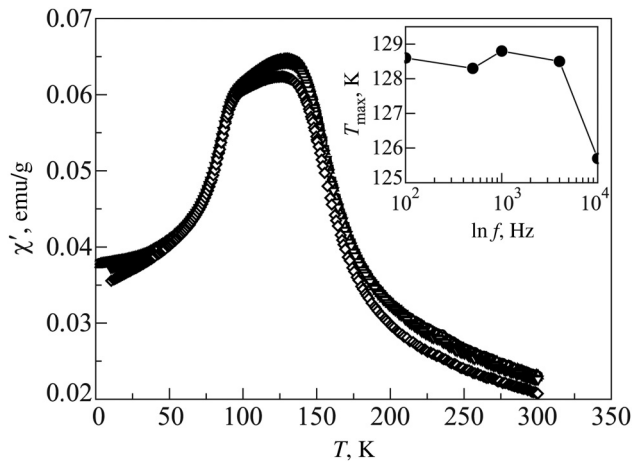
Fig. 3. Temperature dependences of the real part of the dynamic magnetic susceptibility χ' of the $Bi_{95.69}Mn_{3.69}Fe_{0.62}$ sample, measured in an alternating magnetic field of 15 Oe at frequencies of 100 (◯), 500 (☐), 1000 (△), 4000 (▽) and 10000 (◇) Hz. The inset shows the temperature of the maximum as a function of the logarithm of frequency.

frequency of the alternating field. It has been determined that in spin glasses, the maximum is displaced to lower temperatures as the frequency decreases.[12–14]

Figure 3 shows the temperature dependences of the dynamic susceptibility $\chi'(T)$ for the $Bi_{95.69}Mn_{3.69}Fe_{0.62}$ sample, measured in an alternating magnetic field of 15 Oe at frequencies ranging from 100 Hz to 10 KHz. It is evident that even for magnetic susceptibility measurements in weak magnetic fields, instead of a break in $\chi'(T)$, as is typical for spin glasses,[14–16] we observe a washed out maximum. The inset shows the temperature of the maximum T_{max} versus the logarithm of the frequency. Up to ~4 kHz, T_{max} is almost independent of the frequency, and then sharply decreases with an increase in f to 10 kHz. Such behavior differs from what is observed in spin glasses, where T_{max} linearly shifts toward higher temperatures, as frequency increases.[15,16,18,20,21]

Depending on the preparation technique for the BiMn samples, the coercive force H_c can assume values in the range of 1.5 to 15 kOe at room temperatures.[6,7,11] Figure 4 shows the magnetic-field dependences of the $Bi_{95.69}Mn_{3.69}Fe_{0.62}$ magnetization at different temperatures. It is clearly visible that at 300 K there is a hysteresis region with a coercive force of about 2 kOe, which fits the aforementioned range. At the same time, the hysteresis practically disappears at lower temperatures.

Figure 5 shows the temperature dependence of the coercive force. Above 200 K, a significant rise in its magnitude is observed, whereas at low temperatures of 77 and 5 K, $H_c \approx 0.074$ kOe, and is practically independent of temperature. This behavior is characteristic of the previously studied BiMn solid solutions and is explained by the fact that below 90 K, the magnetic anisotropy constant changes signs (anisotropy changes from easy-axis at high temperatures to easy-plane at low temperatures),[6,11,22–23] accompanied by a spin-reorientation transition. We also note that in spin glasses, below the temperature of the maximum at susceptibility, the coercive force shows a sudden increase with a decreasing temperature.[20–21] In our case, as shown above, the
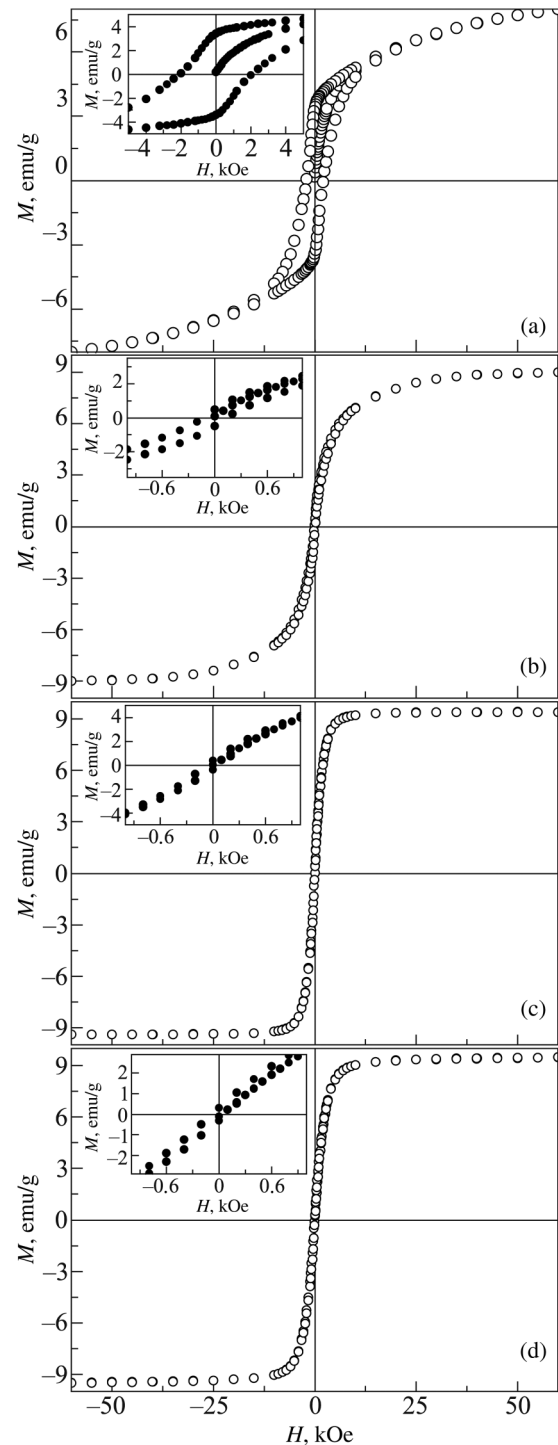

Fig. 4. Magnetic-field dependences of the $Bi_{95.69}Mn_{3.69}Fe_{0.62}$ magnetization, measured at temperatures of 300 (a), 200 (b), 77 (c) and 5 (d) K. The insets show the starting regions of the $M(H)$ curves.

magnitude of H_c at low temperatures is very small and is practically independent of temperature.

As such, neither the differences between the $M(T)$ dependences for the ZFC and FC regimes in weak magnetic fields, nor the $M(H)$ dependences for our samples can be explained by a transition to the spin glass state. Most likely, these phenomena are explained by the changes in anisotropy constants that occur below 90 K. In addition, we cannot exclude the possibility that individual α-BiMn phase inclusions can behave as superparamagnetic clusters at low temperatures.
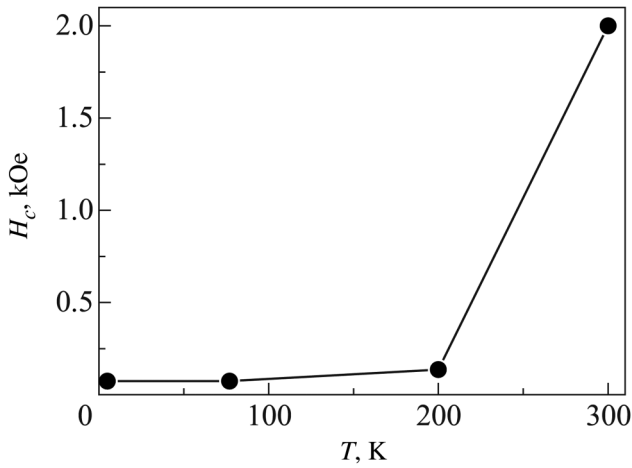
Fig. 5. Temperature dependence of the coercive force H_c in $Bi_{95.69}Mn_{3.69}Fe_{0.62}$..

Resistivity studies

Figure 6 shows measurements of the $\rho(T)$ dependence in the absence of a magnetic field, and in magnetic fields up to 140 kOe, for two directions **H ∥ I** [Fig. 6(a)] and **H ⊥ I** [Fig. 6(b)]. In the absence of a magnetic field, the ratio $\rho(300\,K)/\rho(4.2\,K) \approx 7.5$, whereas $\rho(300\,K) \approx 450\ \mu Ohm\cdot cm$. At the same time, the value $\rho(300\,K)/\rho(4.2\,K)$ in pure bismuth can be nearly two orders of magnitude higher and $\rho(300\,K) \approx 40\text{-}140\ \mu Ohm\cdot cm$.[24–28] For Bi–Te, Bi–Sb alloys the ratio is $\rho(300\,K)/\rho(4.2\,K) \approx 10$ for 2at% concentrations of Te and $\rho(300\,K)/\rho(4.2\,K) \approx 8.3$ for 0.1at% concentrations of Sb.[27] With further increases in the concentration of Sb and Te, the ratio of the electrical resistivities decreases even further. The $\rho(300\,K)/\rho(4.2\,K)$ ratio for our $Mn_{3.69}Bi_{95.69}Fe_{0.62}$ sample, as well as the higher value of
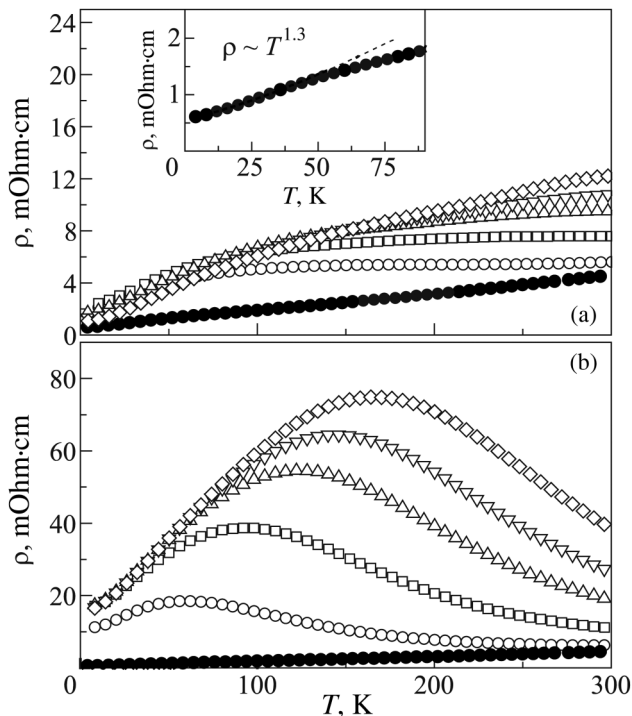

Fig. 6. Specific electrical resistivity as a function of temperature in the absence of a magnetic field (●) and in magnetic fields H, kOe: 10 (○), 30 (□), 60 (△), 90 (▽) and 140 (◇) for directions **H ∥ I** (a) and **H ⊥ I** (b).

$\rho(300\,K)$, can be attributed to the presence of the additional magnetic α-BiMn phase and individual iron atoms. In the absence of an external magnetic field, one observes a metallic behavior of $\rho(T)$, analogous to that of pure bismuth [25,29,30] wherein the resistivity decreases with a lowering of the temperature ($d\rho/dT > 0$). A detailed analysis of this dependence shows a small kink above 50 K. In the temperature range of 5-50 K, the electrical resistivity is well described by a $\rho \sim T^{1.3}$ dependence, whereas above 50 K and up to 300 K one observes a linear dependence $\rho \sim T$ [inset Fig. 6 (a)]. At the same time, as was shown in Refs. 25 and 30, it is possible to observe pronounced $\rho(T)$ anomalies (appearance of maxima, or the dependence becomes semiconductor-like) even with relatively low level additions of impurity atoms. It is also known that at low temperatures, the presence of magnetic atoms can also often lead to an appearance of a minimum along the temperature dependence, related to charge carrier scattering by magnetic atoms (Kondo effect).[31–33] In our case, the role of magnetoactive centers can be played by iron atoms and inclusions of the α-BiMn phase. At the same time, there are no such anomalies along the $\rho(T)$ of the studied materials, whereas the presence of a metallic behavior across the entire temperature range indicates that in the absence of a magnetic field, the main contribution to conductivity comes from the bismuth phase. Refs. 26 and 28 show that with a decreasing temperature, the linear region of $\rho(T)$ for pure bismuth can be observed all the way down to 12 K. Data from other authors[27] show that this boundary temperature is slightly higher and can reach approximately 25 K. At even lower temperatures, pure bismuth shows $\rho \sim T^n$ where the exponent n changes from 2 to 2.75, depending on the study. If the high-temperature linear dependence is sufficiently easily explained by the standard model of electron-phonon scattering,[27,34] then there is still no unambiguous interpretation that can be applied to the low-temperature dependence. According to earlier studies, the $\rho \sim T^2$ power dependence is explained either the appearance of a specific electron-phonon scattering mechanism that is native to bismuth and some other semimetals (intervalley electron-phonon scattering),[27] or by electron-hole scattering processes.[26,27] In our case, as we showed above, just as in pure bismuth, there are two temperature regions with different dependences $\rho(T)$. However, the linear region ends at a much higher temperature of about 50 K, whereas for lower temperatures $\rho \sim T^n$ with $n = 1.35$, which differs from the pure bismuth exponent. We attribute this to the additional impact the α-BiMn magnetic phase has on the conductivity.

Turning on the magnetic field leads to a noticeable change in the character of $\rho(T)$, and the electrical resistivity increases significantly. In the case when **H ∥ I** [Fig. 6(a)], the electrical resistivity decreases with decreasing temperature. In the region of 100 K, the figure shows a sort of crossover, where the rate of resistivity decrease ramps up significantly, and when the field increases, so does the crossover temperature, and the entire effect washes out. The **H ⊥ I** dependences have an entirely different behavior [Fig. 6(b)]. The resistivity increases with decreasing temperature and reaches a maximum at T_p, at which point it decreases down to liquid helium temperatures, i.e. with a decrease in temperature one observes an insulator-metal transition (IMT) along $\rho(T)$. The

value of $\rho_{H\perp I}$ (300 K) / $\rho_{H\|I}$ (300 K) $\approx$ 1.1 and 3.1 for fields of 10 kOe and 140 kOe, respectively, and $\rho_{H\perp I}$ (5 K) / $\rho_{H\|I}$ (5 K) $\approx$ 5. 3 and 16.5 for fields of 10 and 140 kOe. These ratios suggest that the anisotropy of the test compound properties increases, as the temperature decreases.

With a decrease in temperature for the **H** $\perp$ **I** direction, all of the $\rho(T)$ curves for magnetic fields higher than 10 kOe gradually converge on a single line with a metallic resistance behavior. At low temperatures, the $\rho(T)$ dependences for different magnetic fields practically coincide, and only at higher temperatures can one observe a deviation from the "general" $\rho(T)$ dependence. In other words, at low temperatures, the rate of increase in the specific resistance of $Bi_{95.69}Mn_{3.69}Fe_{0.62}$ is the same at all applied magnetic fields as the temperature increases. With an increase in temperature, one observes a sudden decrease in the rate of $\rho(T)$ increase at various applied magnetic fields (a sort of a crossover). Additionally, with an increase in the applied external field, the starting temperature for this sharp change in the $\rho(T)$ rate of increase also rises. The same trend is observed for the **H** $\perp$ **I** direction, but with a large spread in ρ values. Such resistivity behavior correlates with the magnetization temperature dependence, which gradually saturates below 100 K for fields above 30 kOe.

The behavior of $\rho(T)$ in magnetic fields is somewhat different from what was observed earlier when discussing pure bismuth, for which, according to Ref. 35, there can also be peaks along $\rho(T)$ in a magnetic field, though as the temperature decreases, those curves do not converge on a single line, as is the case for our samples, and as the field increases they shift parallel to each other to higher fields. Moreover, the temperatures of the maxima are also different from those observed in pure bismuth. According to the data in Ref. 35, at 90 kOe, $T_p \approx$ 90 K, whereas in our case $T_p \approx$ 144 K.

Figure 7 shows the temperature T_p of the $\rho(T)$ maximum as a function of the magnetic field in the **H** $\perp$ **I** configuration. T_p rises with an increasing magnetic field and gradually saturates. In our case $T_p \sim H^{0.37}$.

Figure 8 shows the temperature dependences of relative magnetoresistance $\Delta\rho/\rho_0 = [\rho(H) - \rho(H = 0)]/\rho(H = 0)$ for **H** $\|$ **I** (a) and **H** $\perp$ **I** (b). In both cases, starting at room temperature, the magnetoresistance rises with decreasing temperature

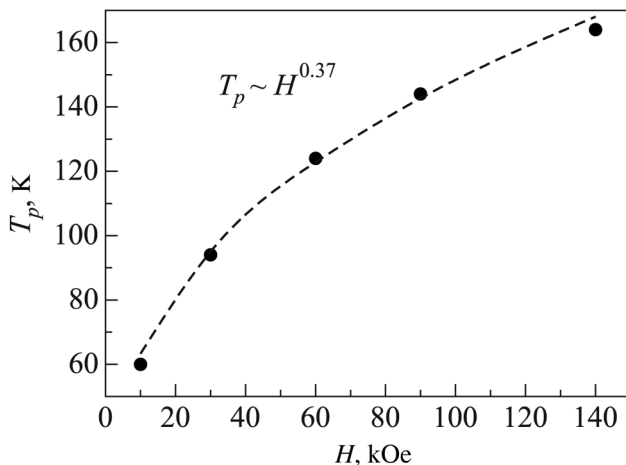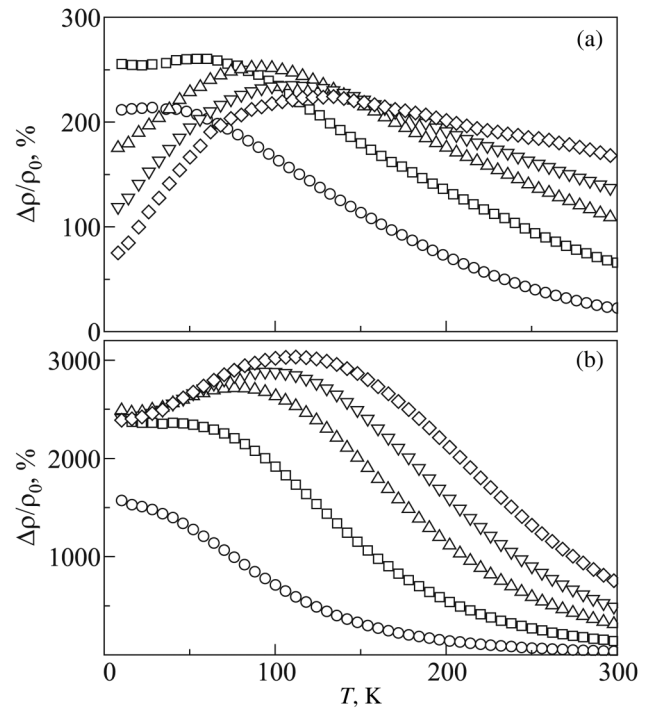Fig. 8. Temperature dependences of the relative magnetoresistance $\Delta\rho/\rho_0$ in the magnetic fields of 10 (O), 30 ($\square$), 60 ($\triangle$), 90 (∇) and 140 ($\Diamond$) kOe along the **H** $\|$ **I** (a) and **H** $\perp$ **I** (b) directions.

(positive magnetoresistance), and at temperatures below 100 K it either plateaus in small fields (10 and 30 kOe) or shows a maximum in fields above 30 kOe. The figure also makes it clear that the behavior of the $\Delta\rho/\rho_0$ dependences differs qualitatively with increasing fields for the **H** $\|$ **I** and **H** $\perp$ **I** cases. For a more detailed discussion, Fig. 9 plots the $\Delta\rho/r_0$ values obtained at maxima temperatures as a function of the magnetic field for **H** $\|$ **I** and **H** $\perp$ **I**. It is worth noting that for the **H** $\perp$ **I** direction, the value of the relative magnetoresistance increases monotonically with an increasing field, up to $\Delta\rho/\rho_0 \approx$ 3033% at 140 kOe with a slowing in the rate of increase at higher magnetic fields. At the same time, along **H** $\|$ **I** one observes a non-monotonic behavior of the $\Delta\rho/\rho_0$ (H) dependence: there is a rise until 30 kOe ($\Delta\rho/\rho_0 \approx$ 261%) which is followed by a fall to $\Delta\rho/\rho_0 \approx$ 224% at 140 kOe.

The divergences in the behavior of the $\Delta\rho/\rho_0$ (T) and $\Delta\rho/\rho_0$ (H) dependences for different magnetic field

Fig. 7. Dependence of the $\rho(T)$ maximum temperature T_p on the magnetic field along the **H** $\perp$ **I** direction.
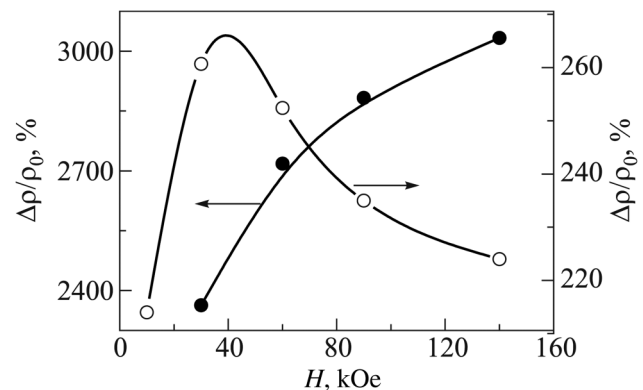

Fig. 9. Magnetic-field dependences of the relative magnetoresistance $\Delta\rho/\rho_0$. The $\Delta\rho/\rho_0$ values were taken at temperatures of the maxima on the $\Delta\rho/\rho_0$ dependences along the **H** $\perp$ **I** ($\bullet$) and **H** $\|$ **I** (O) directions.

configurations suggest a strong anisotropy of our samples' magnetic properties. It is also worth noting that in contrast to our case, in pure bismuth the magnetoresistance is a few orders of magnitude higher in good samples (low content of structural defects and impurities).[24,36,37]

According to modern theory, bismuth possesses a relatively complex band structure. The Fermi surface consists of three highly elongated electron regions that are close to ellipsoids and one hole ellipsoid of revolution. The Fermi energy is about few hundredths of an electron volt. Any external perturbations (temperature, magnetic field, deformations etc.) can affect the degree of electron-hole overlap, and the kinetic properties (resistivity, in our case) as a result. For example, in the case of electron and hole Fermi surface overlap, one observes a metal-insulator transition, along with possible intermediate states.[1,2] Ref. 38 shows that in bismuth, even at relatively small fields (up to 30 kOe), when measuring along the selected directions, phenomena similar to a magnetic breakdown (quantum tunneling of charge carriers in a magnetic field between two energy bands) can be observed.

As was shown above, in our case, in the absence of the magnetic field at low temperatures, the dependence is $\rho \sim T^{1.3}$ and is different from that of pure bismuth, which most often shows as $\rho \sim T^2$.[27,28] We note that magnon scattering often gives rise to the $\rho \sim T^2$ dependence.[39,40] We do not see this dependence in our case, which can indicate an absence of such scattering processes despite the presence of magnetic inclusions of the α-BiMn phase. Additionally, the studied materials show $T_p \sim H^{0.37}$, whereas bismuth shows $T_p \sim H^{0.45}$.[35] In pure bismuth and other nonmagnetic semimetals [35,41] there is an observable link between ρ_0 and T_p: $\rho_0 \sim T^n$, $T_p \sim H^{1/n}$. Such differences in the electroresistivity behavior relative to pure bismuth can be related to the impact the α-BiMn phase magnetism and the external magnetic field have on the conductive properties of our sample. This influence can cause certain changes in the degree of electron-hole overlap of the Fermi surface, and as a result change the number of different types of charge carriers (electrons and holes) as well as their associated motion. All of this introduces a significant correction to the resistivity behavior of the studied material in comparison to pure bismuth. A change in the magnetic field angle relative to the crystallographic directions can lead to an additional change in the degree of electron-hole overlap, and to both a deviation of the electroresistivity behavior from the already existing one in the absence of a magnetic field, and to an onset of a strong anisotropy of the electro- and magnetoresistance temperature dependences observed during our measurements. This explanation correlates nicely with the multi-band theory explanation of the bismuth anomalies.[42]

In parallel, it is important to not exclude other mechanisms that lead to an anomalous electroresistivity behavior. For example, a change in the magnetic structure of the α-BiMn phase below 100 K can lead to an onset of a significant magnetostriction, and to a change in the conductive properties of the $Bi_{95.69}Mn_{3.69}Fe_{0.62}$ material as a result. To check the validity of this mechanism, we will conduct magnetostriction measurements in the near future.

We also do not exclude other more exotic mechanisms that could cause the onset of an insulator-metal transition along the $\rho(T)$ curve in a magnetic field, such as the appearance of a so-called Bose metal state, which contains coexisting excitonic and superconducting instabilities.[35,43,44]

In conclusion, we note that in the near future we are also planning to measure magnetic-field dependences of electroresistivity at different temperatures, which should enable a more detailed investigation of electroresistivity behavior features in magnetic fields. Measurements of the Hall effect are equally important, and can give information on a series of questions, regarding the interactions between charge carriers from different sub-bands in a magnetic field, similar to what has been done in Refs. 41 and 42. A large interest exists in a theoretical and experimental study of the band-structure changes in bismuth, which take place in Bi-Mn solid solutions during temperature decreases and under the action of magnetic fields having different orientations.

Conclusions

1. It is determined that the studied solid solution has a composition 95.69 at%Bi, 3.69 at%Mn and 0.69 at%Fe and contains two phases – the bismuth matrix and α-BiMn inclusions. It is also textured.

2. It is shown that the anomalous behavior of the magnetization temperature dependence is related to the reorientation transition of the Mn magnetic moments in the α-BiMn phase below ≈100 K (for $T \leq 100$ K) that happens due to the changes in the magnetic anisotropy constants with decreasing temperature. This is confirmed by the results of the studies on the dynamic susceptibility and magnetic-field dependences of magnetization.

3. It is determined that the $\rho(T)$ dependence of the $Bi_{95.69}Mn_{3.69}Fe_{0.62}$ alloy in a magnetic field behaves non-monotonically, whereas the dependence is monotonic in the absence of the field.

4. It is shown that the magnetoresistance is positive over the entire range of temperatures, however the behavior of the magnetoresistance as a function of temperature is qualitatively different for the different orientations of the magnetic field $\mathbf{H} \parallel \mathbf{I}$ and $\mathbf{H} \perp \mathbf{I}$. The magnetoresistance is about an order of magnitude higher along the $\mathbf{H} \perp \mathbf{I}$ direction, than along $\mathbf{H} \parallel \mathbf{I}$, and reaches 3033% in a magnetic field of 140 kOe.

5. Anomalous behavior of the electroresistivity temperature dependence in the absence and presence of various magnetic fields, can be explained by a change in the degree of electron-hole Fermi surface overlap due to the influence of the α-BiMn phase magnetism and the acting external magnetic field.

6. We also present a theory that the change in the angle of the magnetic field could lead to a variation in the degree of electron and hole overlap along different directions, resulting in the onset of anisotropy.

a)Email: terekhov.andrii@gmail.com

---

[1]L. A. Fal'kovskii, Phys. Usp. **11** 1–21 (1968).

[2]V. S. Edel'man, Phys. Usp. **20** 819–835 (1977).

[3]Om Prakash, Anil Kumar, A. Thamizhavel, and S. Ramakrishnan, Science **355**, 52 (2017).

[4]P. Lejay, P. de Rango, A. Sulpice, B. Giordanengo, R. Tournier, R. Retoux, S. Deslandes, C. Michel, M. Hervieu, and B. Raveau, Rev. Phys. Appl. **24**, 485 (1989).

[5]N. B. Brandt, E. A. Svistova, Yu. G. Kashirskii, and L. V. Lyn'ko, Sov. Phys. *JETP* **29**, 3 (1969).

[6]Yong-Sheng Liu, Jin-Cang Zhang, Zhong-Ming Ren, Min- An Gu, Jing-Jing Yang, Shi-Xun Cao, and Zheng-Long Yang, Chin. Phys. Lett. **27**, 0975024–1 (2010).

[7]N. V. Rama Rao, A. M. Gabay, and G. C. Hadjipanayis, J. Phys. D **46**, 062001 (2013).

[8]V. N. Svetlov, A. V. Terekhov, V. B. Stepanov, A. L. Solovjov, E. V. Khristenko, O. M. Ivasishin, A. D. Shevchenko and Z. D. Kovalyuk, Low Temp. Phys. **41**, 314 (2015).

[9]Katsunari Oikawa, Yoshifuru Mitsui, Keiichi Koyama, and Koichi Anzai, Mater. Transact. **52**, 2032 (2011).

[10]F. Yin, N. Gu, T. Shigematsu, and N. Nakanishi, J. Mater. Sci. Technol. **12**, 335 (1996).

[11]J. B. Yang, W. B. Yelon, W. J. James, Q. Cai, M. Kornecki, S. Roy, N. Ali, and Ph. l'Heritier, J. Phys. Condens. Matter **14**, 6509 (2002).

[12]K. Binder and A. P. Young, Rev. Mod. Phys. **58**, 801 (1986).

[13]I. Ya. Korenblit, E. F. Shender, Phys. Usp. **32** 139–162 (1989);

[14]H. Kawamura, and T. Taniguchi, *Handbook of Magnetic Materials*. Spin Glasses **24**, Elsevier, Amsterdam (2015).

[15]I. G. Deac, J. F. Mitchell, and P. Schiffer, Phys. Rev. B **63**, 172408 (2001).

[16]Y. Wang and H. J. Fan, Phys. Rev. B **83**, 224409 (2011).

[17]P. E. Jönsson, Adv. Chem. Phys. **128**, 191 (2004).

[18]V. A. Desnenko, A. I. Rykova, V. A. Sirenko, A. V. Fedorchenko, A. S. Cherny, E. N. Khatsko, and A. V. Eremenko, Low Temp. Phys. **38**, 206 (2012).

[19]A. I. Rykova, A. V. Terekhov, A. S. Cherny, E. N. Khatsko, and A. V. Yeremenko, Low Temp. Phys. **38**, 529 (2012).

[20]A. Haldar, K. G. Suresh, and A. K. Nigam, EPL **91**, 67006 (2010).

[21]J. Dho, W. S. Kim, and N. H. Hur, Phys. Rev. Lett. **89**, 027202 (2002).

[22]B. W. Roberts, Phys. Rev. **104**, 607 (1956).

[23]Tu Chen and W. E. Stutius, IEEE Trans. Magn. **10**, 581 (1974).

[24]P. Kapitza, Proc. R. Soc. London A **119**, 358 (1928).

[25]A. B. Focke and J. R. Hill, Phys. Rev. **50**, 179 (1936).

[26]G. K. White and S. B. Woods, Philos. Mag. **3**, 342 (1957).

[27]V. Chopra, R .K. Ray, and S. M. Bhaga, Phys. Status Solidi A **4**, 205 (1971).

[28]C. A. Kukkonen and K. F. Sohnt, J. Phys. F **7**, L193 (1977).

[29]G. W. C. Kaye, Proc. R. Soc. London A **170**, 561 (1939).

[30]N. Thompson, Proc. R. Soc. London A **155**, 111 (1936).

[31]W. J. de Haas, J. de Boer, G. J. van dën Berg, Physica **1**, 1115 (1934).

[32]J. Kondo, Prog. Theor. Phys. **32**, 37 (1964).

[33]A. A. Abrikosov, *Fundamental theory of metals*, Nauka, Moscow (1987).

[34]E. H. Sondheimer, Proc. Phys. Soc. A **65**, 561 (1952).

[35]Y. Kopelevich, J. C. Medina Pantoja, R. R. da Silva, and S. Moehlecke, Phys. Rev. B **73**, 165128 (2006).

[36]F. B. Jewett, Phys. Rev. I **16**, 51 (1903).

[37]P. B. Alers and R. T. Qebber, Phys. Rev. **91**, 1060 (1953).

[38]Yu. A. Bogod and E. E. Eremenko, JETP Lett. **3**, 113 (1966).

[39]E. A. Turov, FMM **6**, 203 (1958).

[40]S. V. Vonsovski, *Magentism*, Nauka, Moscow (1971).

[41]J. Xu, D. E. Bugaris, Z. L. Xiao, Y. L. Wang, D. Y. Chung, M. G. Kanatzidis, and W. K. Kwok, Phys. Rev. B **96**, 115152 (2017).

[42]Xu Du, Shan-Wen Tsai, D. L. Maslov, and A. F. Hebard, Phys. Rev. Lett. **94**, 166601 (2005).

[43]Y. Kopelevich, J. H. S. Torres, R. R. da Silva, F. Mrowka, H. Kempa, and P. Esquinazi, Phys. Rev. Lett. **90**, 156402 (2003).

[44]D. Das and S. Doniach, Phys. Rev. B **64**, 134511 (2001).

Translated by CWS